ORGANIZATION OF RESISTIVITY EXPLORATION DATA FOR DEVELOPMENT OF DEEP GEOTHERMAL SYSTEMS - REPROCESSING MAGNETOTELLURIC DATA FROM THE KAKKONDA GEOTHERMAL FIELD, NORTHEAST JAPAN

Yusuke Yamaya[1], Toshihiro Uchida[2], Yasuo Ogawa[3] and Toru Mogi[4]

[1]Renewable Energy Research Center, Fukushima Renewable Energy Institute, AIST,
2-2-9 Mchiike-dai, Koriyama, Fukushima 963-0298, Japan

[2] Geological Survey of Japan, National Institute of Advanced Industrial Science and Technology (AIST),
1-1-1 Higashi, Tsukuba, Ibaraki 305-8567, Japan

[3] Volcanic Fluid Research Center, S5-13, Tokyo Institute of Technology, 2-12-1 Ookayama, Meguro, Tokyo 152-8551, Japan

[4] Laboratory of Global Resources and Environmental System, Division of Sustainable Resources Engineering,
Faculty of Engineering, Hokkaido University, N13W8 Kita-ku, Sapporo, Hokkaido 060-8628, Japan

y.yamaya@aist.go.jp

Keywords: *magnetotellurics, resistivity, thermal structure, supercritical geothermal system, Kakkonda geothermal field.*

ABSTRACT

To determine a drilling target for deep geothermal systems, one should know the distribution of subsurface temperature and fluids. The resistivity structure estimated by electromagnetic explorations represented by magnetotellurics (MT) includes such information. However, there are non-unique relationships between rock resistivity and temperature or fluid content. We started to organize pre-existing data including resistivity structures and borehole logs to estimate temperature and fluid content at the target depth. In 1995, the deep geothermal drilling project at the Kakkonda geothermal field, northeast Japan, completed the WD-1 well, which reached a Quaternary granite intrusion with a temperature of 500°C at a depth of 3700 m;. MT surveys were conducted in this field in 1994, 1996, and 1998 to estimate the 3-D resistivity structure. The central part of the granite was found to be a strong conductor, which was interpreted as a saline-fluid-rich zone. However, in the resistivity structure, we did not find clear boundaries at high temperatures of the fluid-rich zone. The technical limitations in analysis at the time can be considered one of the reasons for such broad resistivity boundaries. To more accurately resolve the resistivity structure, we applied the latest analyzing technique to the previous MT data and obtained effective results. In this paper, we report these results and integrated them with other geophysical and geological data to further interpret the subsurface environment.

1. INTRODUCTION

Recently, expectations for utilizing supercritical geothermal resources, which commonly exist deeper in the crust than conventional shallow geothermal reservoirs, have been raised and we are now at the stage for test drillings at several potential areas. The Iceland Deep Drilling Project (IDDP) reached a supercritical geothermal system with a temperature of 427°C at a depth of 4627 m in 2017 (IDDP-DEEPEGS2, 2017). To effectively utilize such deep geothermal resources to generate electric power, one has to correctly know the subsurface temperature and fluid content. The resistivity structure estimated by electromagnetic explorations represented by magnetotellurics (MT) includes such information. However, non-unique relationships between rock resistivity and temperature or fluid content sometimes make it difficult to interpret resistivity structure. Therefore, a need exists to accumulate and organize known data including resistivity structure, well logs and laboratory experimental results. For example, some studies have attempted to apply machine learning methods including artificial intelligence (AI) to find relationships among these data. In this study, as the first step of the organization of known data, we reprocessed previous MT data from the Kakkonda geothermal field to accurately estimate the resistivity structure in and around the Kakkonda high temperature granite intrusion.

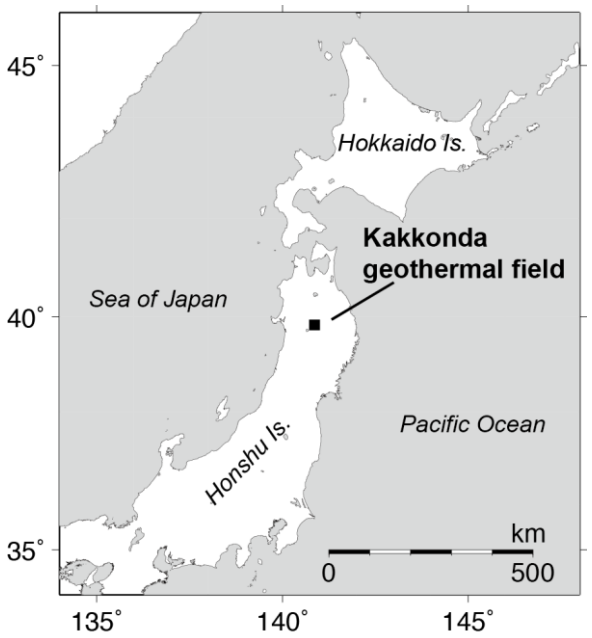

Figure 1: Location of the Kakkonda geothermal field.

2. KAKKONDA GEOTHERMAL FIELD

2.1 Overview

The Kakkonda geothermal field is on northeastern Honshu Island, Japan (Figure 1). Utilizing the shallow (conventional) hot-water-dominated geothermal system, the power plant has an installed capacity of 80 MWe. A deeper

portion of the reservoir is associated with the fracture systems, which were created by the intrusion of Quaternary granite (Doi et al. 1998). The granite is very young, less than 0.3 Ma, and is thought to be the heat source of the reservoir system. The New Energy and Industrial Technology Development Organization (NEDO) drilled a deep research well, WD-1, at the northwestern edge of the production zone. The WD-1 well reached the Quaternary granite which as a temperature of more than 500°C at 3729 m depth (Doi et al. 1998; see Figure 6).

2.2 Previous magnetotelluric study

Wideband MT data were collected by NEDO and the Geological Survey of Japan (GSJ) in 1994, 1996 and 1998. The data included full impedance tensors at all the stations and at some stations magnetic transfer functions. Uchida et al. (2000a; 2000b) and Uchida et al. (2003) developed two- and three-dimensional (2- and 3-D) resistivity structure models, respectively, applying inversion analysis to these data. The main features of these models were as follows: 1) shallow low-resistivity layers over almost the entire study area, 2) a large high-resistivity body at approximately 1 km depth on the western part, and 3) low-resistivity layers below the high-resistivity body, except for the deep high-resistivity body on the eastern part.

The estimated boundaries of the granite rock and fluid rich zone were not sharp but gradually varied in resistivity. If the boundaries are actually sharp, there is a need to improve the resolution of the resistivity model to better decide the drilling target of the deep geothermal system. Some issues remained in the previous 2-D and 3-D analysis. Uchida et al. (2000b) suggested that the 2-D analysis in this area could not correctly estimate the deep structure because of a strong 3-D effect. In addition, the 3-D analysis used only the off-diagonal components of the impedance tensor (Uchida et al. 2003). However, Siripunvaraporn et al. (2005a) reported that using the on-diagonal components was effective to estimate a precise 3-D structure. Therefore, the previous resistivity model of the study area still had room for improvement, which can be achieved with common procedures of the present day as computational technology has developed considerably since the early 2000s.

3 THREE-DIMENSIONAL RESISTIVITY MODEL

3.1 Modeling

The 3-D inversion analysis of the obtained MT data was conducted using the 3-D inversion program WSINV3DMT (Siripunvaraporn et al. 2005b; Siripunvaraporn and Egbert, 2009). Data for 14 frequencies between 0.0022 and 30 Hz from the 100 stations were used. The input data contained four components of the impedance tensor. The 3-D calculation region consisted of cuboid cells and had dimensions of 52, 70, and 30 cells in the x (north), y (east), and z (vertical) directions, respectively. The minimum cuboid cell was designed to have a horizontal 150 m square base with a vertical thickness of 50 m. The common initial and prior models, which defined a uniform resistivity of 100 Ωm, were used. The root-mean-square (RMS) residuals of the observed and calculated responses were 5.07 in the initial model, allowing for a 5% error floor. The inversions reduced the RMS residuals to 1.47 after four iterations. Figure 3 shows comparisons of the calculated and observed data. Figures 4 and 5 show the estimated resistivity structure model.

3.2 Results and Interpretation

The estimated 3-D resistivity structure was characterized by a wide spreading conductive layer shallower than 1 km, conductive bodies C1 and C2, and resistive bodies R1 and R2 (Figures 4 and 5). Although these anomalies basically corresponded to those found in the previous 2-D and 3-D models (Uchida et al. 2000a; Uchida et al. 2000b and Uchida et al. 2003), their structural boundaries were sharpened compared to those of the previous models. Such sharpness was probably a result of using the diagonal components of the impedance tensor and the fine grid design.

The shallow conductive layer, which corresponds to a temperature less than 200°C, is interpreted as a cap rock overlying the shallow geothermal reservoir, and as an aquifer of hot springs. C2 is the underlying the cap rock, which corresponds to the production zone of the geothermal power plant, indicates the geothermal reservoir. R1 is a middle resistive zone, which corresponds to dacite intrusions. The geological correspondence to R2 is unclear and further study is needed. C1, which is in the central part of the Kakkonda granite, is the most important conductor in this study. Because C1 is estimated to be below 3 km depth and its surrounding temperature is higher than 500°C, C1 is considered to be a supercritical fluid rich zone. These interpretations are shown in Figure 6 with superimposed geological and thermal structures after Doi et al. (1998). To ensure these interpretations, further validation of the model and resistivity condition in the rocks should be completed.

4. CONCLUSION

In this study, we reprocessed previous MT data from the Kakkonda geothermal field and developed a 3-D resistivity model, which better explained the existing data. This resistivity model corresponded well with the thermal and geological structures (Figure 6). The center of the granite intrusion was estimated to be a conductive zone, which implied the existence of supercritical geothermal fluids, considering the depth and high temperature. However, this inversion analysis did not include the topographic effect and the magnetic transfer function data. In future, we should take these into account to develop a more robust and constrained model. Such an accurate model can be used with the AI model to better estimate thermal structure and supercritical fluid content.

ACKNOWLEDGEMENTS

The authors thank NEDO for the MT field data from the Kakkonda geothermal field.

REFERENCES

Doi, N., Kato, O., Ikeuchi, K. Komatsu, R., Miyazaki, S., Akaku, K., Uchida, T.: Genesis of the plutonic-hydrothermal system around quaternary granite in the kakkonda geothermal system, Japan. *Geothermics*, 27, pp. 663– 690 (1998)

IDDP-DEEPEGS2: The drilling of the Iceland Deep Drilling Project geothermal well at Reykjanes has been successfully completed. The report of the IDDP-2 Completion websites (2017).

Siripunvaraporn, W., Egbert, G., Uyeshima, M.: Interpretation of two-dimensional magnetotelluric profile data with three-dimensional inversion: synthetic examples. *Geophys. J. Int.*, 160, pp. 804–814 (2005a).

Siripunvaraporn, W., G. Egbert, Y. Lenbury, M. Uyeshima: Three-dimensional magnetotelluric inversion: Data-space method, *Phys. Earth Planet. Inter.*, 150, pp. 3–14 (2005b).

Siripunvaraporn, W., G. Egbert: WSINV3DMT: Vertical magnetic field transfer function inversion and parallel implementation. *Phys. Earth Planet. Inter.*, 173, pp. 317–329 (2009).

Uchida, T., Ogawa, Y., Takakura, S., Mitsuhata, Y.: Geoelectrical investigation of the Kakkonda geothermal field, northern Japan. *Proceedings World Geothermal Congress 2000*, pp. 1893–1898 (2000a).

Uchida, T., Ogawa, Y., Takakura, S., Mitsuhata, Y., 2000b, Magnetotelluric investigation on reservoir structure of the Kakkonda geothermal field, northern Japan. *Rept. Geol. Surv. Japan*, 284, pp. 207-220 (in Japanese with English abstract; 2000b).

Uchida, T., Lee, T. J., Cerv, V.: 3-D inversion of magnetotelluric data in the Kakkonda geothermal field, northern Japan, *Proceedings of 6th SEGJ International Symposium*, pp. 274–280 (2003).

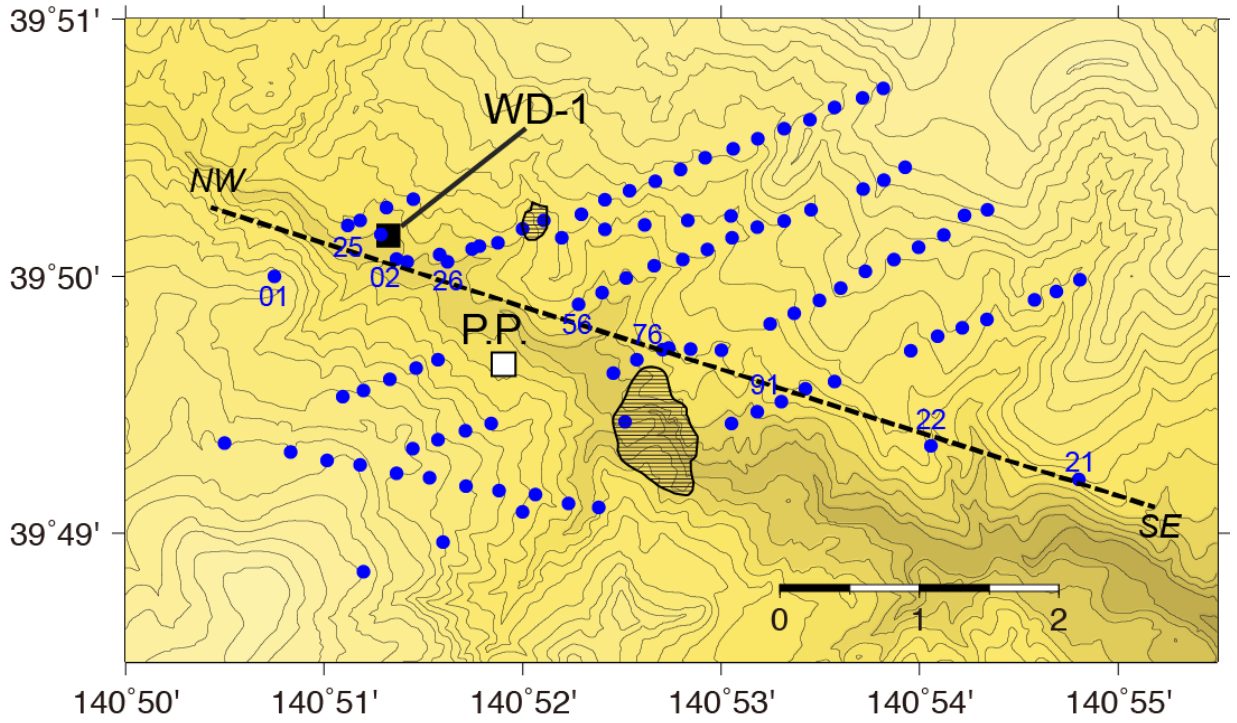

Figure 2: Location map of the Kakkonda geothermal field. Blue circles indicate the magnetotelluric stations. Black square indicates the well WD-1. White square indicates the Kakkonda geothermal power plant. Shaded areas correspond to dacitic intrusions after Doi et al. (1998). Dashed line indicates the profile of the resistivity section shown in Figure 6.

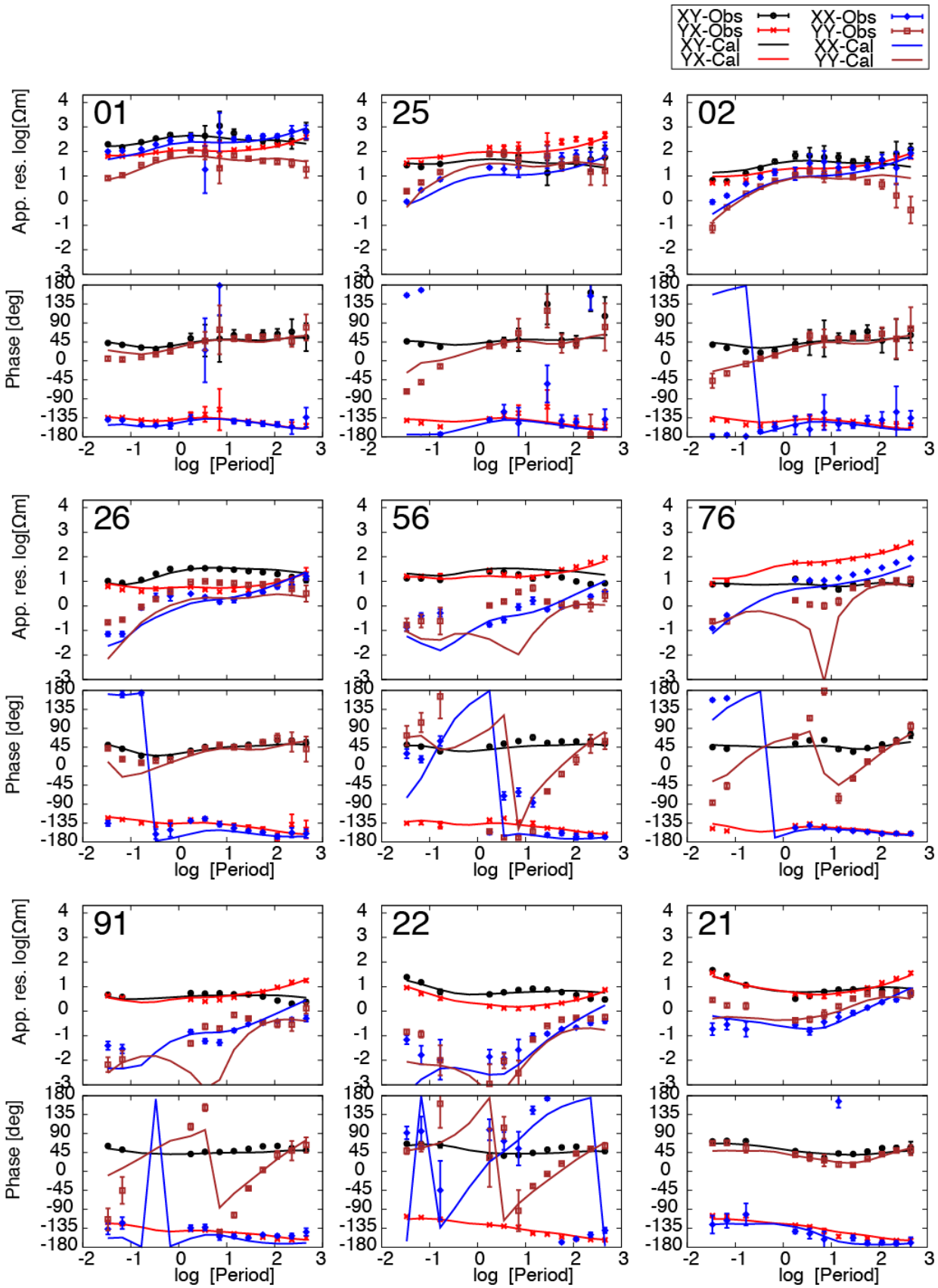

Figure 3: Observed and calculated sounding curves of the apparent resistivity and impedance phase at the stations along the NW-SE profile.

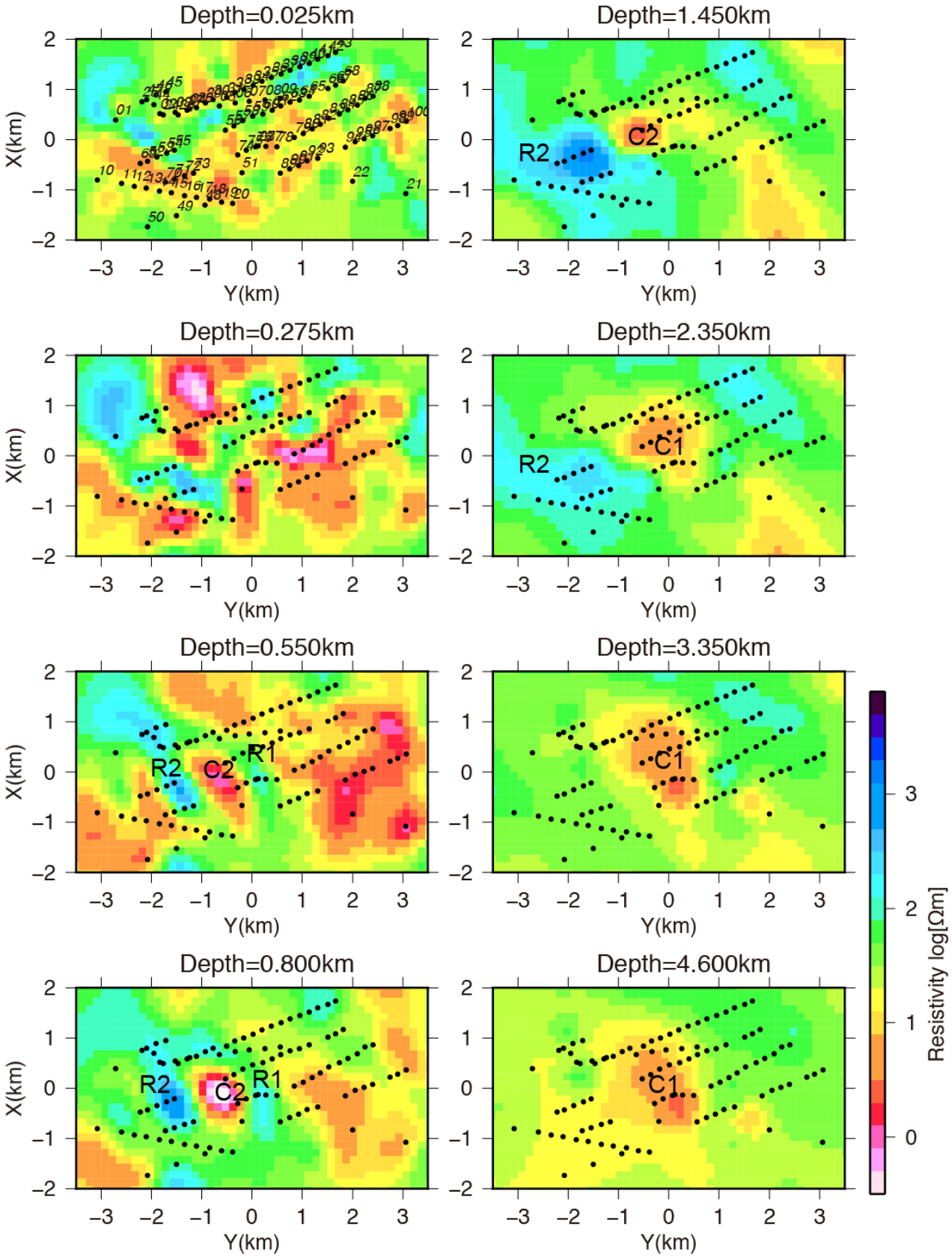

Figure 4: Plane views of the inverted resistivity model at each depth.

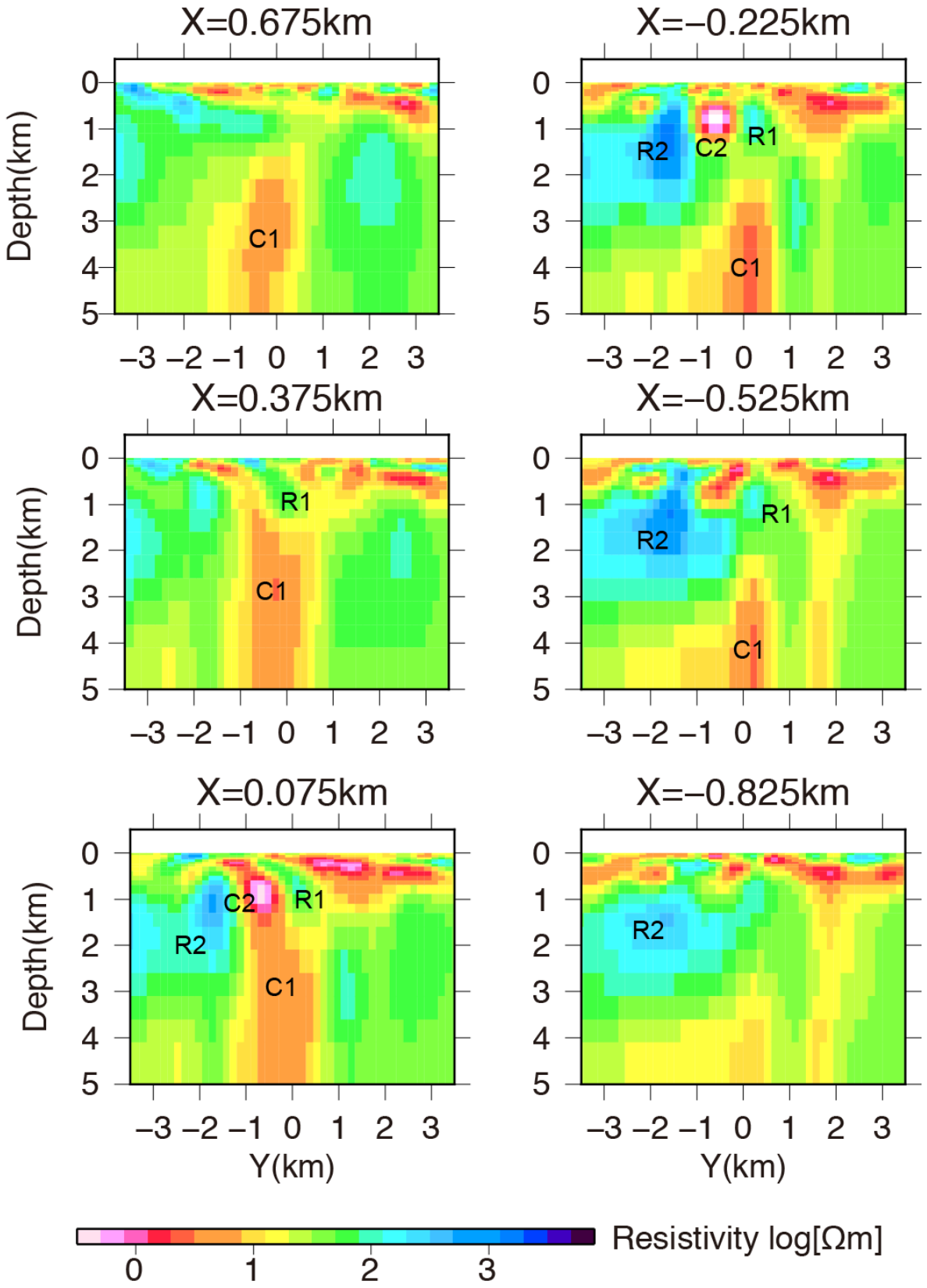

Figure 5: East-West section views of the inverted resistivity model.

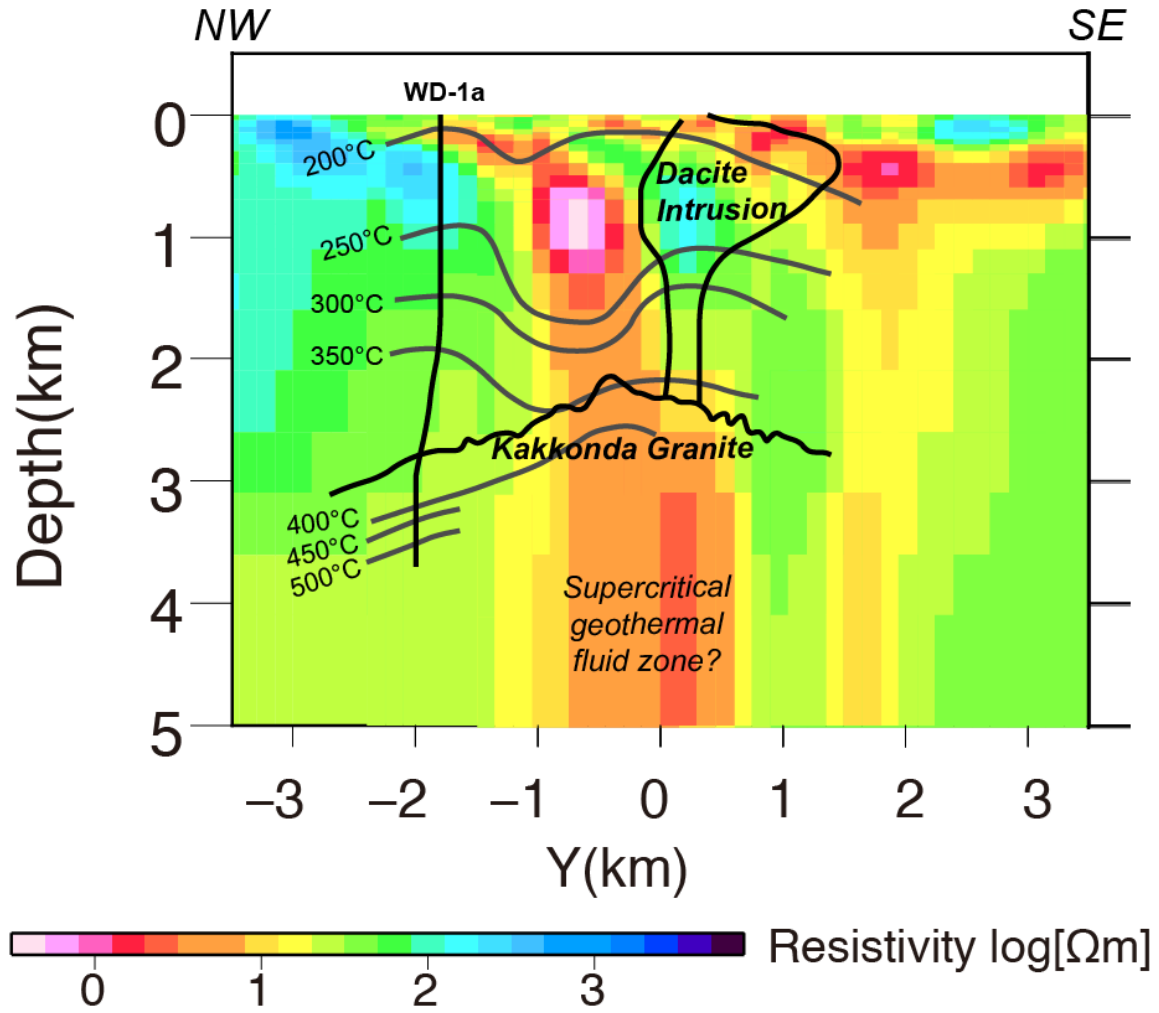

Figure 6: Resistivity section along the NW-SE profile (shown in Figure 2). Geological boundary, thermal structure and well path were reproduced after Doi et al. (1998).